

Electron scattering from krypton: High-resolution experiments and *B*-spline *R*-matrix calculations

This content has been downloaded from IOPscience. Please scroll down to see the full text.

2012 J. Phys.: Conf. Ser. 388 012008

(<http://iopscience.iop.org/1742-6596/388/1/012008>)

View [the table of contents for this issue](#), or go to the [journal homepage](#) for more

Download details:

IP Address: 134.21.16.139

This content was downloaded on 22/10/2014 at 13:51

Please note that [terms and conditions apply](#).

Electron scattering from krypton: High-resolution experiments and *B*-spline *R*-matrix calculations

O. Zatsarinny¹, K. Bartschat¹, and M. Allan²,

¹Department of Physics and Astronomy, Drake University, Des Moines, Iowa 50311, USA

²Department of Chemistry, University of Fribourg, 1700 Fribourg, Switzerland

E-mail: oleg.zatsarinny@drake.edu, klaus.bartschat@drake.edu,
michael.allan@unifr.ch

Abstract. In a joint experimental and theoretical effort, we carried out a detailed study of e-Kr collisions. For elastic scattering and excitation of the $4p^55s$ states, we present total and angle-differential cross sections over the entire angular range ($0^\circ - 180^\circ$) for a number of energies, as well as energy scans for selected angles. The experimental results are in very satisfactory agreement with predictions from fully relativistic Dirac *B*-spline *R*-matrix models.

1. Introduction

Electron scattering from the noble gases is an important problem in the field of atomic collisions. Numerous experimental and theoretical studies have been performed, both for fundamental as well as practical reasons. The detailed study of the many near-threshold resonance features [1] has proven to be very challenging to both experiment and theory alike, and it represents a sensitive test of the quality of any theoretical model. A reliable knowledge of absolute elastic cross sections for rare gases is very important for applications in plasma and discharge physics.

The present work was motivated by the desire to test our newly developed, fully relativistic Dirac *B*-spline *R*-matrix (DBSR) model [2] in detail over extended energy and angular ranges. This has become possible due to significant progress in experimental techniques that allow for scanning the entire angular region $0^\circ - 180^\circ$, measuring at energies down very close to threshold with an energy resolution of better than 15 meV.

2. Experiment

Electrons emitted from a hot filament were energy-selected by a double hemispherical monochromator and focused onto an effusive beam target, introduced by a 0.25 mm nozzle kept at about 30°C . A double hemispherical analyzer for detection of elastically or inelastically scattered electrons ensured background-free signals [3]. Absolute cross sections were determined by comparison against He using a relative-flow method [4]. A specially designed magnetic angle changer allowed for measurements up to 180° scattering angle [5]. The angular acceptance was limited to $\pm 1.5^\circ$ at 10 eV, with an estimated uncertainty in the angular position of $\pm 2^\circ$. The angular acceptance increases with decreasing energy approximately as $E^{-1/2}$, down to an energy of about 1 eV, where it reaches about $\pm 5^\circ$. It remains approximately constant below that. Procedures for ensuring reliable cross sections were described in detail elsewhere [6, 7]. The confidence limit (two standard deviations) for the absolute cross sections is generally about

$\pm 15\%$, although it degrades to about $\pm 25\%$ at energies below 1 eV. The incident electron resolution was ≈ 13 meV at a beam current of ≈ 400 pA.

3. Theory

Since different physical effects are important for elastic scattering and electron impact excitation in the energy range we are interested in, we performed calculations in two different models.

3.1. Elastic Scattering

Away from Feshbach resonances, the most important effect for elastic scattering is the polarization of the target by the projectile. We therefore generalized the non-relativistic two-state (ground state plus one pseudo state) approach employed by Bell *et al* [8] to a fully relativistic framework. Our DBSR_{pol} model only included the $4s^2 4p^6$ ground state with total electronic angular momentum $J = 0$ and a single pseudostate $|\psi_p\rangle$ with $J = 1$ constructed from the configurations $4s^2 4p^5 \bar{5}s$, $4s^2 4p^5 \bar{4}d$, and $4s 4p^6 \bar{5}p$, respectively. This pseudostate, and the corresponding pseudoorbitals $\bar{5}s$, $\bar{5}p$, and $\bar{4}d$, can be defined by the requirement that the static dipole polarizability of the atomic state $|\psi_0\rangle$ be expressed as

$$\alpha = 2 \frac{|\langle \psi_0 | D^{(1)} | \psi_p \rangle|^2}{E_p - E_0}, \quad (1)$$

where $D^{(1)}$ is the dipole operator while E_0 and E_p are the total energies of the ground state and the polarized pseudostate, respectively. $|\psi_p\rangle$ is a normalized solution of the equation

$$(H - E_0)|\psi_p\rangle = D^{(1)}|\psi_0\rangle, \quad (2)$$

with energy

$$E_p = \langle \psi_p | H_{\text{at}} | \psi_p \rangle, \quad (3)$$

where H_{at} is the target Hamiltonian [9]. Our pseudostate yielded a dipole polarizability of $17.3 a_0^3$, where $a_0 = 0.529 \times 10^{-10}$ m is the Bohr radius. This is in very good agreement with the most recent recommended value of $17.075 a_0^3$ [10, 11].

3.2. Inelastic Scattering

An important aspect of our approach is the use of *non-orthogonal, term-dependent* sets of radial functions for each individual state, also accounting for term mixing due to the spin-orbit interaction. The DBSR69 model used for the present work is an extension of the DBSR31p model that was described in [12]. However, instead of the polarized pseudostate that was included in the model to represent the ground-state polarizability for elastic scattering, we added additional physical states in the expectation of better describing the resonance structure in the vicinity of the lowest few excitation thresholds. Specifically, we included all the states of principal configurations $4p^6$, $4p^5 5s$, $4p^5 5p$, $4p^5 4d$, $4p^5 6s$, $4p^5 7s$, $4p^5 6p$, $4p^5 4d$, and $4p^5 4f$, respectively. All valence spinors were generated through a *B*-spline bound-state close-coupling calculation using a number of Kr^+ states with frozen core orbitals. The latter also included states with only one electron in the $4s$ orbital. Consequently, the core-valence correlation, inner-core correlation, the strong term-dependence of the valence orbitals, and the very strong configuration mixing between the $4p^4(n+1)s$ and $4p^4 nd$ states were all treated fully *ab initio*.

We used the published BSR code [13] and our newly developed DBSR program [2] to solve the $(N+1)$ -electron collision problem. The essential idea is to expand the basis of continuum orbitals used to describe the projectile electron inside the *R*-matrix box, i.e., the region where the problem is most complicated due to the highly correlated motion of $N+1$ electrons, also in

terms of a B -spline basis. A semi-exponential grid for the B -spline knot sequence was set up to cover the inner region up to the R -matrix radius of $a = 50 a_0$, where $a_0 = 0.529 \times 10^{-10} \text{m}$ is the Bohr radius. We employed 111 B -splines to span this radial range. With up to 313 scattering channels included, interaction matrices with dimensions of about 80,000 needed to be diagonalized. This was achieved by a parallelized version of the DBSR code.

We calculated partial-wave contributions up to $J = 51/2$ numerically. With such a high value of J , no extrapolation scheme to account for contributions from even higher partial waves was necessary for all observables presented in this paper. The cross sections of interest were then calculated in the same way as in the standard R -matrix approach.

4. Results and Discussion

Due to space limitations, we can only present a few selected results here. More details can be found in recent publications [14, 15]. Below we show some total cross sections, as well as angular scans at fixed energy and energy scans at fixed angle for both elastic and inelastic collisions.

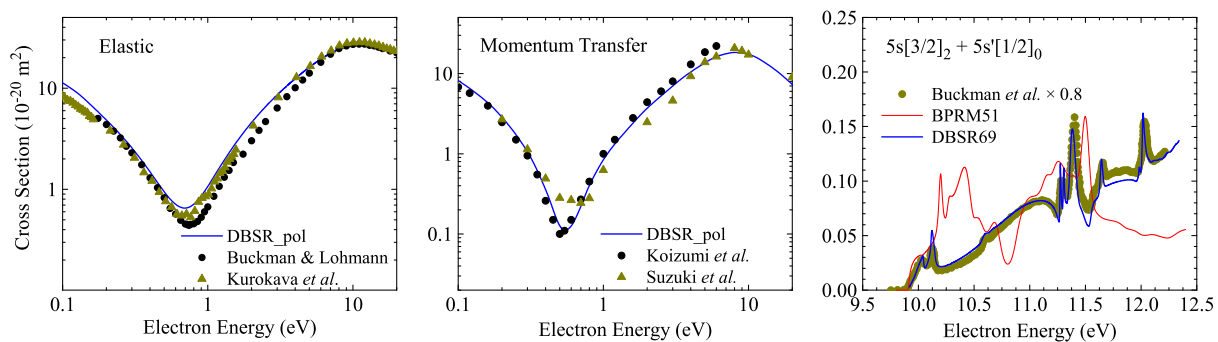


Figure 1. Angle-integrated elastic (left), momentum-transfer (center), and metastable production cross section (right) for electron collisions with Kr. The absolute experimental data for elastic collisions are from [16-19]. The Breit-Pauli R -matrix results [20], were obtained with the standard Belfast R -matrix code. The published experimental data of Ref. [21] were visually renormalized to the DBSR-69 results.

Figure 1 displays the angle-integrated elastic and momentum transfer cross sections, as well as the excitation function for the production of metastable excited Kr atoms in the $(4p^5 4s)^3 P_{2,0}$ states. The DBSR69 elastic and momentum-transfer results are in excellent agreement with the experimental data shown, although there are datasets in the literature with significant scatter. After renormalizing the published data of Buckman *et al* [21] by a factor of 0.8 (which is within the experimental uncertainty), we obtain excellent agreement in the metastable excitation function as well. Clearly DBSR69 is a vast improvement over the earlier BPRM51 model [20].

Figures 2 and 3 exhibit results for elastic scattering, once as a function of the scattering angle for fixed energies of 2 eV and 8 eV, and once as a function of the energy for fixed scattering angles of 90° and 180° . The overall agreement between the independently normalized, absolute experimental data and the DBSR_pol predictions is very satisfactory. A few small differences remain, in particular regarding the depth of the minimum in the energy at 180° .

Figure 4 displays the DCS for electron impact excitation of the four states with dominant configuration $4p^5 5s$ as a function of energy for two fixed scattering angles. Overall, we judge the agreement between the present measurements and the DBSR69 predictions as very satisfactory. While the agreement between experiment and theory is certainly not perfect, the magnitude problems noted earlier in comparison with the data of Phillips [23] are essentially resolved. We emphasize again that the present experimental data were normalized *independently* of the present theory by cross-normalization to the well-known elastic DCS for e-He collisions.

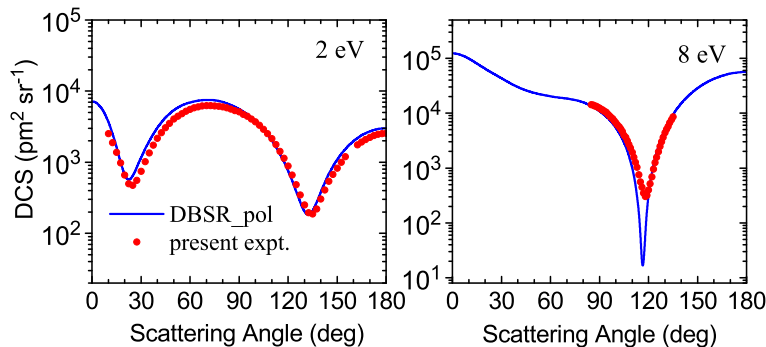


Figure 2. Differential cross section for elastic e–Kr scattering at electron energies of 2 eV and 8 eV as a function of the scattering angle. Our experimental data are compared with the DBSR_pol predictions.

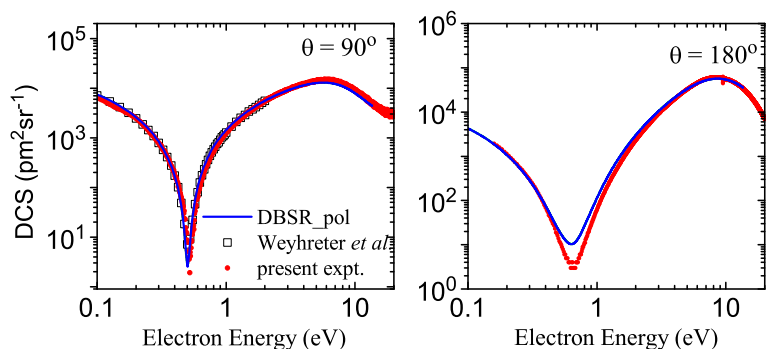


Figure 3. Differential cross section for elastic e–Kr scattering at angles of 90° and 180° as a function of the projectile energy. Our experimental data are compared with the DBSR_pol predictions. For $\theta = 90^\circ$, we also show the experimental data of Weyhreter *et al* [22].

The largest remaining discrepancies between experiment and the DBSR69 predictions occur very close to threshold, in particular at the extreme angle of 180°. This problem is almost certainly related to drifts of the detector response function very close to threshold, which did not “see” the very low-energy electrons after the excitation process.

The other difference worth mentioning is that the theoretical results are lower than the experiment in the 12–14 eV energy range, in particular at 180°. Interestingly, the discrepancy occurs only for the $5s'[1/2]_1$ and $5s[3/2]_1$ states. This difference is very unlikely due to instrumental problems. Even if drifts caused imprecision of the instrumental response function (for which all spectra were corrected), such a problem would necessarily apply to all final states at a given scattering angle, since the spectra were recorded in an “interleaved” manner [15].

Figure 5 shows the corresponding results as a function of the scattering angle for a fixed incident projectile energies of 15.0 eV. We plot our DCS data for the seven angles at which we ran energy scans together with earlier experimental data [24, 25]. Given the good agreement of our measurements with those of Trajmar *et al* [24] and the theoretical predictions, we suspected a normalization error in the data published by Guo *et al* [25]. This error was indeed confirmed, and the published latter data should be multiplied by a factor of 0.37 [26].

The comparison of our previous 47-state semi-relativistic Breit-Pauli (BSR47) [12] and the current DBSR69 results 15 eV show very good agreement. This gives us confidence in the proper treatment of both relativistic effects and channel coupling. Small differences between the two sets of predictions primarily occur near the backward direction, where the theoretical description seems to become more sensitive to the details of the computational model. This emphasizes the usefulness of having experimental data available for comparison over the *entire* angular range, but particularly at 180°.

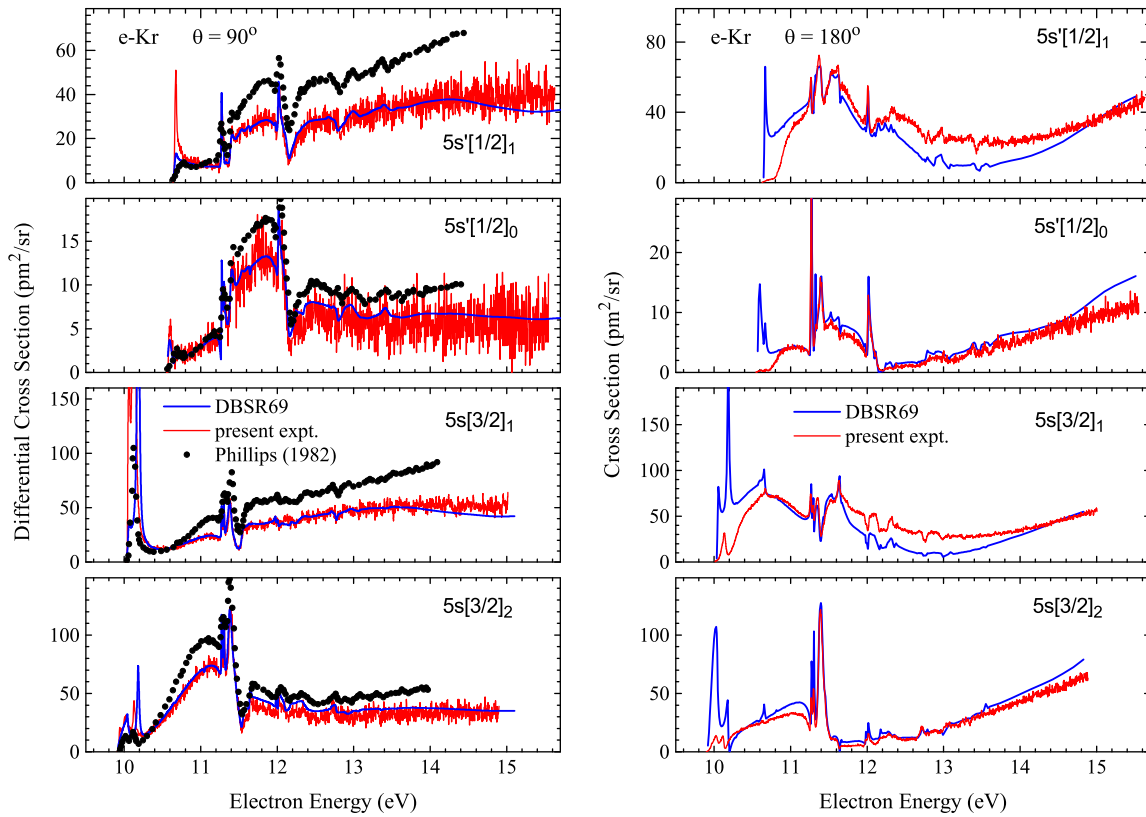


Figure 4. Differential cross section for electron-impact excitation of Kr at scattering angles of 90° and 180° . The experimental data (ragged lines) are compared with theoretical predictions from the DBSR69 model. For 90° , we also show the experimental data of Phillips [23].

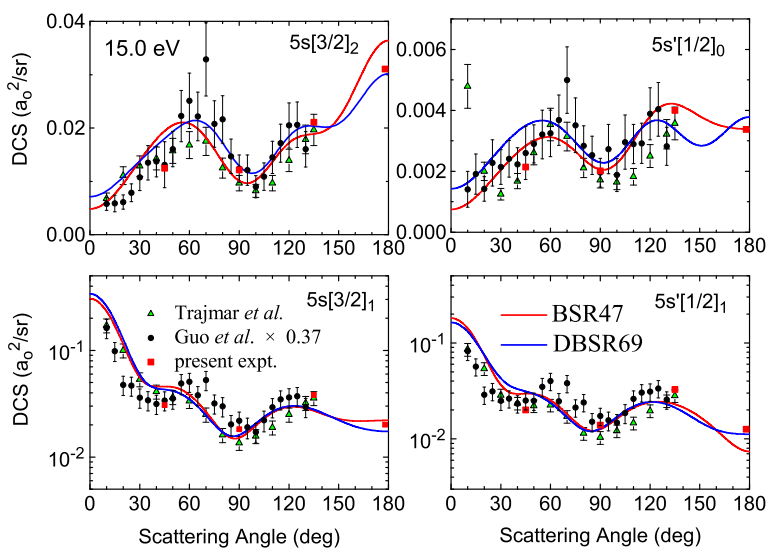


Figure 5. Differential cross section for electron-impact excitation of the four states in the $4p^55s$ manifold of Kr at an incident projectile energy of 15.0 eV. The experimental data are compared with theoretical predictions from the DBSR69 model and the semi-relativistic BSR47 calculations [12]. Also shown are the experimental data of Trajmar *et al* [24] and of Guo *et al* [25]. The latter were multiplied by 0.37 in order to fix a normalization error in [26].

5. Conclusions

We have presented results from a joint experimental and theoretical study of electron scattering from Kr. For elastic scattering, the computational model, DBSR_{pol}, included only two states, namely the ground state and a dipole polarized pseudostate that yields a dipole polarizability of $17.3 a_0^3$. Based on the excellent agreement with a variety of measurements, this relatively simple, but fully relativistic and *ab initio* model appears to be sufficient for an accurate description of low-energy elastic scattering, reproducing most of both the energy and angle dependence of the DCS. In the future, we will use this model for the other heavy noble gases Ne, Ar, and Xe. In particular, we plan to calculate angle-integrated elastic as well as momentum transfer cross sections. The latter are critical ingredients to simulate energy transport phenomena in plasmas.

For electron impact excitation of the $4p^5 5s$ states of Kr, very satisfactory agreement between our absolute, high-resolution experimental data and predictions from a fully-relativistic DBSR69 model was obtained, resolving likely normalization problems in previous experimental work. The success of the DBSR69 model gives us confidence in applying it to the even more complicated problem of e–Xe collisions and to compare the results with experimental benchmark data. A joint project for this system is currently in progress.

Acknowledgments

We thank H. Hotop for encouraging us to carry out this work and for many stimulating discussions, and M.A. Khakoo for investigating the suspected problem with the data published in [25]. This work was supported by the United States National Science Foundation under grants #PHY-0757755, #PHY-0903818, and the TeraGrid allocation TG-PHY090031, and by the Swiss National Science Foundation (project No. 200020-131962).

References

- [1] Buckman S J and Clark C W 1994 *Rev. Mod. Phys.* **66** 539–655
- [2] Zatsarinny O and Bartschat K 2008 *Phys. Rev. A* **77** 062701
- [3] Allan M 1992 *J. Phys. B: At. Mol. Opt. Phys.* **25** 1559
- [4] Nickel J C, Zetner P W, Shen G and Trajmar S 1989 *J. Phys. E: Sci. Instrum.* **22** 730
- [5] Allan M 2000 *J. Phys. B: At. Mol. Opt. Phys.* **33** L215
- [6] Allan M 2005 *J. Phys. B: At. Mol. Opt. Phys.* **38** 3655–3672
- [7] Allan M 2007 *J. Phys. B: At. Mol. Opt. Phys.* **40** 3531–3544
- [8] Bell K L, Berrington K A and Hibbert A 1988 *J. Phys. B: At. Mol. Opt. Phys.* **21** 4205–4216
- [9] Burke P G and Mitchell J F B 1974 *J. Phys. B* **7** 665
- [10] Holm U and Kerl K 1990 *Mol. Phys.* **69** 803
- [11] 2010 <http://ctcp.massey.ac.nz/dipole-polarizabilities>
- [12] Hoffmann T H, Ruf M W, Hotop H, Zatsarinny O, Bartschat K and Allan M 2010 *J. Phys. B* **43** 085206
- [13] Zatsarinny O 2006 *Comp. Phys. Commun.* **174** 273
- [14] Zatsarinny O, Bartschat K and Allan M 2011 *Phys. Rev. A* **83** 032713
- [15] Allan M, Zatsarinny O and Bartschat K 2011 *J. Phys. B* **44** 065201
- [16] Buckman S J and Lohmann B 1987 *J. Phys. B* **20** 5807
- [17] Kurokawa M, Kitajima M, Toyoshima K, Odagiri T, Kato H, Kawaharaand H, Hoshino M, Tanaka H and Ito K 2010 *Phys. Rev. A* **82** 062707
- [18] Koizumi T, Shirakawa E and Ogawa I 1986 *J. Phys. B* **19** 2331
- [19] Zatsarinny O, Bartschat K and Allan M 1989 *J. Phys. D* **22** 1848
- [20] Bartschat K and Grum-Grzhimailo A N 2000 *J. Phys. B* **33** 4603
- [21] Buckman S J and Clark C W 1994 *Rev. Mod. Phys.* **66** 539
- [22] Weyhreter M, Barzik B, Mann A and Linder F 1988 *Z. Phys. D.* **7** 333
- [23] Phillips J M 1982 *J. Phys. B: At. Mol. Phys.* **15** 4259–4268
- [24] Trajmar S, Srivastava S K, Tanaka H, Nishimura H and Cartwright D C 1981 *Phys. Rev. A* **23** 2167–2177
- [25] Guo X, Mathews D F, Mikaelian G, Khakoo M A, Crowe A, Kanik I, Trajmar S, Zeman V, Bartschat K, Fontes C J and Grum-Grzhimailo A N 2000 *J. Phys. B* **33** 1895
- [26] Khakoo M A 2010 *private communication*